Int J Adv Manuf Technol (2018) 94:1771–1779
DOI 10.1007/s00170-017-0056-0

ORIGINAL ARTICLE

Simulation of a uniform energy control strategy of single-phase AC resistance spot welding

Kang Zhou[1] · **Ping Yao**[2]

Received: 28 June 2016 / Accepted: 16 January 2017 / Published online: 16 February 2017

Abstract A uniform energy control strategy for single-phase AC resistance spot welding (RSW) was proposed in this paper. Through seriously analyzing the welding process, a variable, which is the product of square of welding current and welding time (I^2t), can be considered as an ideal control variable to ensure the uniform energy delivery. It can be translated to constant current control in reality. However, when the winding ratios of the welding transformer are different, direct translation can obtain incorrect result. Then, the effect of different winding ratios on welding current was studied, and a method which can obtain a corresponding constant welding current when different number of windings were employed was proposed. Final simulation and corresponding analysis validated the proposed method, and the method can be employed to facilitate the current welding production. This work provides a convenient and effective method for welding control when different ratios of welding transformer are employed.

Keywords Resistance spot welding · Constant current control · Winding ratio · Welding transformer

1 Introduction

Resistance spot welding (RSW) is employed extensively in the sheet metal joining industry, especially in automobile, recreational vehicles, railroad passenger cars, office furniture, and some other relative manufacturing areas [1, 2, 3]. However, RSW suffers from a significant problem of inconsistent quality during the process [4, 5]. Proper energy delivery is a significant element to obtain satisfactory welding products, due to that the products are formed by the solid metal absorbing energy and then melting [6]. Though there are two kinds of RSW machines with different types of energy delivery modes—single-phase AC RSW machine and three-phase medium-frequency DC RSW machine—the former type machine is still employed prevalently because of its popularity and simplicity [7, 8].

To obtain uniform welding products for workpieces from one batch, a lot of relative researches have been conducted for decades. Firstly, finite element method (FEM) was employed to seek the variation rules of nugget formation and growth for control system design [9, 10]. However, the governing differential equations cannot precisely predict the heat transfer situation if phase transition phenomenon is involved [1, 11]. Due to the same reason, the method which used the material characteristics to design the control system [12] may also be limited in practice. Also, some particular process variables, such as electrode displacement or velocity, dynamic resistance or electrode force, etc., were employed to establish a uniform nugget growing control system, because they can provide significant information concerning the nugget formation and growth process [13]. The commonly used modeling tools were neural network [14, 15], fuzzy logic [16], or the combination of these two methods [17], or other data fitting methods [18].

Though a lot of methods were employed to establish the models for obtaining uniform welds with satisfactory quality, there is no reliable and reasonable energy delivery mode appearing. Because of the existence of the welding

✉ Kang Zhou
zhoukang326@126.com

[1] State Key Laboratory of High-Temperature Gas Dynamics, Institute of Mechanics, Chinese Academy of Sciences, Beijing 100190, China

[2] College of Electromechanical Engineering, Guangdong Polytechnic Normal University, Guangzhou 510635, China

transformer, which is a step-down transformer, any tiny difference from workpiece to workpiece in the secondary coil may induce large uncertainties in the primary coil and affect a uniform energy delivery. Moreover, mechanical differences between the machines may also affect the uniform energy delivery and nugget growth process.

During the welding process, the workpieces have a lot of individual differences, such as surface roughness and/or variety of contaminations and thickness and/or stack-up variation, even from the same batch products [19]. A uniform energy delivery strategy is important to guarantee a high efficiency of obtaining welding products with satisfactory quality. In recent years, there are a variety of control strategies employed in real welding production, such as constant voltage control (CVC), constant power control (CPC), which is also named as constant energy control (CEC), and constant current control (CCC) [6]. These strategies employed one specific control variable as an approximate constant during the welding process; however, the variable may not be relative to a uniform nugget formation and growth process, and those applications may be limited. For electrical structure of a single-phase AC RSW machine, which is a typical nonlinear and time-varying system, the individual machine difference may also seriously affect the uniformity of nugget formation and growth. Hence, a uniform energy delivery strategy should be introduced in reality in order to guarantee a uniform nugget growing process under any individual machine condition, and it should be induced based on the principle of nugget formation and growth and characteristics of single-phase AC RSW operation.

The goal of this work is to develop an energy control method for realizing the uniform energy delivery. In Sect. 2, the principle of nugget formation and growth will be discussed. Section 3 will focus on the design of a new control strategy. The simulation will be conducted in Sect. 4. Section 5 will provide concluding remarks and suggestions for future works.

2 Principle of nugget formation and growth during single-phase AC RSW process

The energy delivery in single-phase AC RSW is controlled by two parallel silicon-controlled rectifiers (SCRs). The electrical structure and corresponding continuous waveforms of voltage and current of RSW are shown in Fig. 1 [20].

where TR is a welding transformer. The firing angle α, which is also named as trigger time, is a sole control variable during the welding process, while θ is the conduction angle, denoting the effective duration of the welding current. In this work, all of the angles can be translated into corresponding times according to the working frequency of the RSW system. For example, if the frequency of the AC power source is 50 Hz, which means the control frequency of the RSW system is 100 Hz, 90° firing angle corresponds to 5 ms trigger time, so is the conduction angle. It can be obviously found that the zero-crossing point of the welding current is behind the zero-crossing point of the AC power source due to the existence of inductive components in the system. Under this circumstance, we employed ψ, which is the phase lag angle, to denote this deviation.

During the welding process, the metal workpiece melts by the heat energy generated from the interface between two or more workpieces. Hence, the amount of heat energy delivered into the welding system is very important for the process. The energy is generated following the basic Joule heat calculating formula:

$$Q = \int_{T_1}^{T_2} I(t)^2 R(t) dt \tag{1}$$

where Q is the amount of energy generated during the process, T_1 and T_2 respectively denote the beginning and terminating times of the process, $I(t)$ is the welding process, and $R(t)$ is the dynamic resistance of the workpieces. In this equation, welding current $I(t)$ and the welding durations T_1 and T_2 are controlled by a preliminary specific welding schedule. Dynamic resistance $R(t)$ is a unique parameter which can reflect the workpiece characteristics in real time. To obtain a uniform energy delivery for one batch of workpiece, a detailed analysis should be seriously conducted.

After enough heat energy is delivered into the welding system, solid metal melts and liquid nugget forms, and then the workpiece dynamic resistance can be considered as a series of solid metal resistances and liquid metal resistances. To clearly illustrate the nugget formation and growth, the affecting workpieces are divided into single uniform units with the same volume as shown in Fig. 2 [19].

It can be observed that in the direction which is vertical to the direction of the welding current, the units of the metal resistances are in parallel connecting mode. During the welding process, because the contact resistance of two workpieces is the largest in the interface due to the existence of contaminations, the initial melting occurs in the interface and then expands into nearby zones. For each unit, the same amount of energy is needed to melt from solid metal to liquid nugget. Each unit can be considered having the same value of resistance. Then, the issue for obtaining a steady nugget formation and growth process can be translated as guaranteeing each unit obtaining the same amount of energy during the same duration. According to Eq. (1), it can be considered as that during each equal time, the constant current should be guaranteed, in other words, the constant variable in the control should be I^2t, which is a compound variable.

According to this analysis, the CCC may be a more appropriate control strategy to obtain uniform welding products than CVC and CPC, because the welding current I is an important element in that compound variable. However, in the electrical system of a single-phase AC RSW, there is a step-

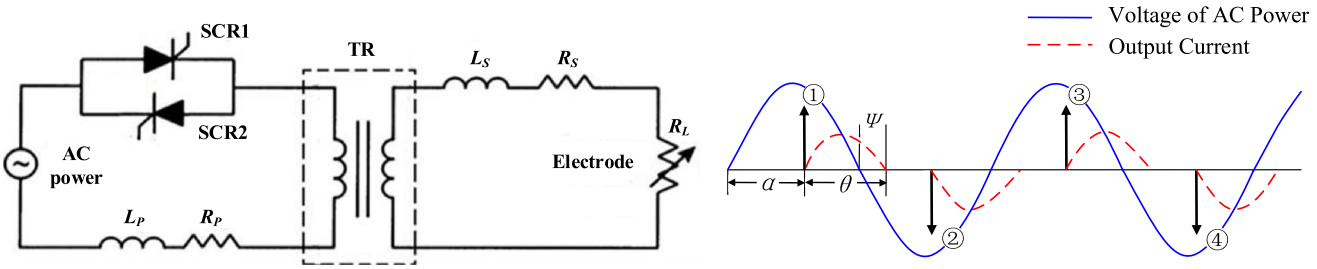

Fig. 1 Schematic figures of electrical structure and corresponding waveforms of voltage and current of RSW

down welding transformer, which makes the welding electrical system a low-voltage high-current system. In practical application, different transformers have different ratios, which make the value of welding current I the same but with a different current effective duration t. The effective duration can be shown as the conduction angle θ in Fig. 1 during one control cycle. The different values of I^2t can make obtaining welds with uniform quality difficult in practice [21].

3 Proposed method

In our previous works, a constant current control algorithm has been proposed and validated by various experiments [22], which was established based on a nonlinear model of electrical system of the RSW machine. Apart from a PD controller which is used to alleviate the influence by difference between positive and negative triggers, the mathematical relation between firing angle and desired welding current can be written as follows:

$$\alpha_{i+1} = \frac{\arccos\left[\frac{I_R^d}{I_{R,i}^a}\cdot[\cos(0.1\pi\alpha_i)-\cos[0.1\pi(10+\psi_i)]]+\cos[0.1\pi(10+\psi_i)]\right]}{(0.1\pi)} \quad (2)$$

where I_R^d is the root mean square (RMS) value of the desired welding current and $I_{R,i}^a$ is the corresponding value of the actual welding current in the i^{th} control cycle; hence, this equation can be used to calculate the firing angle in the $i+1^{\text{th}}$ control cycle based on the actual welding current and other relative information obtained in the i^{th} control cycle.

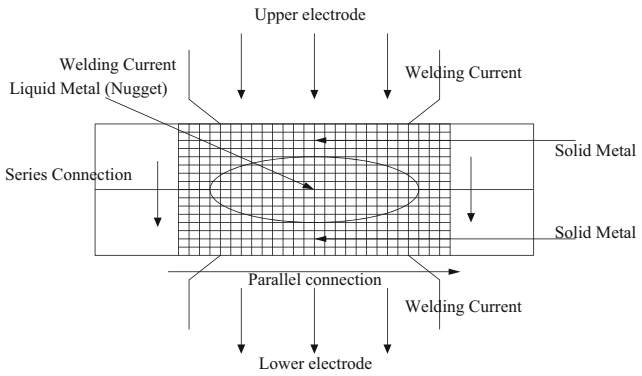

Fig. 2 Workpiece dynamic resistance during the welding process

Though the model can employ CCC strategy, which is the most commonly used energy control strategy [23], just constant current cannot guarantee uniform energy delivery for the workpieces from the same batch, as illustrated in Sect. 2. However, the proper control variable, which is I^2t, is a compound variable. Also, the variable includes t, which is the current effective duration and is directly related to the trigger time α, which is closely relative to the ratios of the welding transformer. In addition, the magnitude of the welding current is very large; hence, larger I^2 may induce larger inconveniences in reality, especially in a digital signal processor (DSP)-controlled device and trigonometric function form of the model. Due to these reasons, it is difficult to directly translate the item I_R^d /$I_{R,i}^a$ to the corresponding form of I^2t.

To solve this problem, an appropriate method can be proposed to translate the welding current to a corresponding value when the ratio of the transformer is changed. Firstly, the effect of the ratio of the welding current on the conduction angle and welding current in the secondary coil should be clearly illustrated. We assume that the welding transformer is an ideal linear transformer. In normal condition, the different ratio of the transformer significantly affects the peak value of the welding current, with other operation conditions unchanged. The larger the peak value of the welding current, the larger the value of current effective duration t induced. As presented in [22, 24], all of the components in the secondary coil of the welding transformer can be transferred into the primary coil, and the integrated electrical working waveform can be depicted as shown in Fig. 3 [22, 24]:

In Fig. 3, R and L denote respectively the equivalent dynamic resistance and inductance of the welding system. Then, the transient equation of the welding current can be written in following form:

$$i(t) = i_1 + i_2 = \frac{\sqrt{2}U}{Z}\left[\sin(\omega t+\alpha-\varphi)-e^{-\frac{\omega t}{\tan\varphi}}\sin(\alpha-\varphi)\right] \quad (3)$$

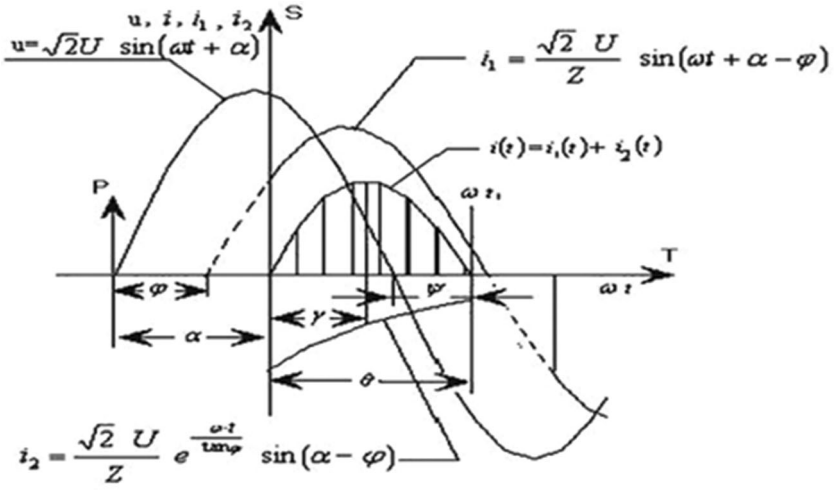

Fig. 3 The integrated electrical working waveform

where $\omega = 2\pi f$ and f denotes the AC power source frequency, $Z = \sqrt{R^2 + (\omega L)^2}$, and $\varphi = \arctan(\omega L/R)$ is the power factor angle, induced by the existence of inductive components in the system. The waveform includes all of the variables during the welding process. Assuming that the welding current reaches its peak value at $\omega t = \gamma$, the peak value can be defined as

$$i(t)_{\max} = \frac{\sqrt{2}U}{Z}\left[\sin(\gamma + \alpha - \varphi) - e^{-\frac{\gamma}{\tan\varphi}}\sin(\alpha - \varphi)\right] \tag{4}$$

As shown in Eq. (4), it is difficult to seek the relation between $i(t)_{\max}$ and θ. Also, obtaining a sophisticated nonlinear description, even using a neural network format does not make sense for practical application. However, intuitively, these two variables are proportional. To obtain a simple relation, numerical simulation was employed. The tool of MATLAB Simulink, which is a popular used tool in reality [25], was employed to seek the relation, as shown in Fig. 4.

In the simulation, two SCRs, which were TH1 and TH2 in Fig. 4, were controlled by two pulse generators with 0.01 s of phase difference. The value range of the trigger time is [0.0035, 0.0075] with 0.0001 increment, which is a commonly used range in reality. After parameter adjustment, there was no full conduction [26], which was 180° of the conduction angle, appearing in this trigger time range. The workpiece resistance and inductance for achieving this goal were respectively 0.0004Ω and $3.84 \times 10^{-7}H$. Some arrays of simulations were conducted. Firstly, the default condition of the welding

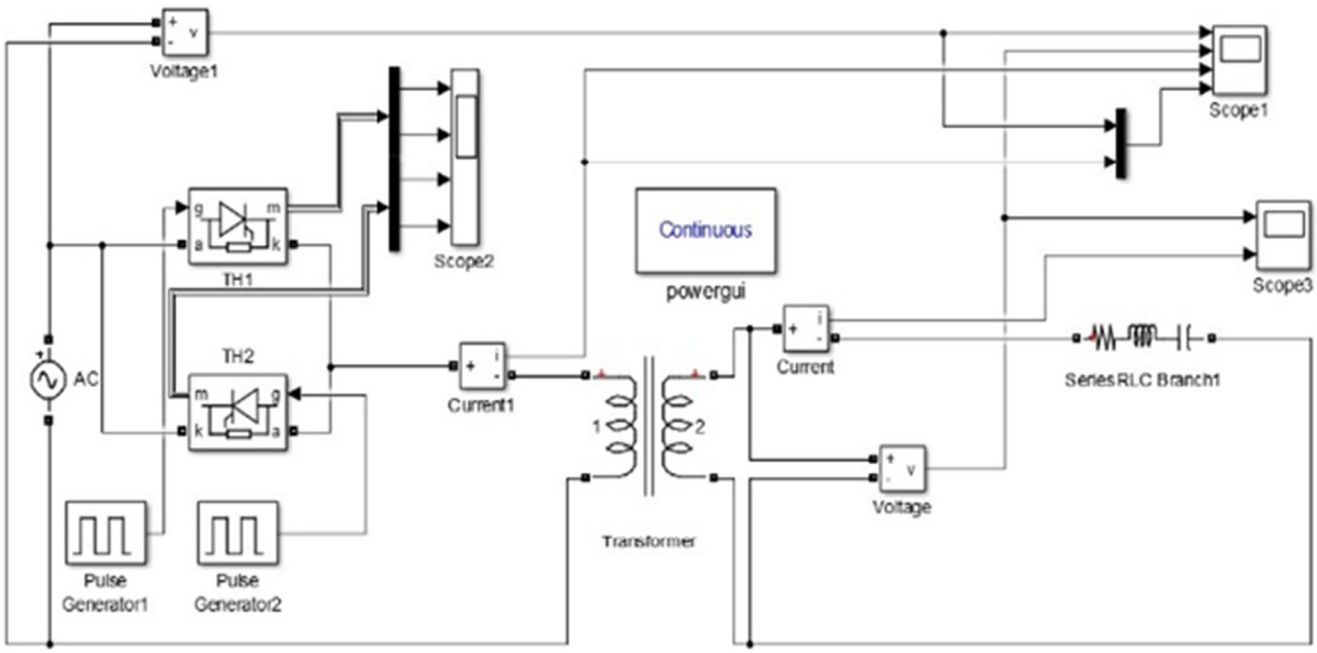

Fig. 4 Schematic figure of the Simulink *flowchart*

transformer was respectively 200,000 and 3000 of winding 1 and winding 2. The relation can be shown in Fig. 5.

According to Fig. 5, the relation of these two variables is approximately linear. To validate this intuition, a linear curve fitting was conducted. The linear curve fitting result can be shown in Fig. 6.

A corresponding mathematical description of curve fitting can be written as follows:

$$\theta = 0.012975 \times I_{\max} + 44.929 \tag{5}$$

To explore the effect of different ratios on the relation between conduction angle and peak value of the welding current, a variety of ratios were employed; corresponding figures are shown in Fig. 7.

Equations (6), (7), (8), (9), (10), (11), (12), and (13) were the corresponding curve fitting mathematical descriptions:

$$\theta = 0.012465 \times I_{\max} + 41.158 \tag{6}$$

$$\theta = 0.012506 \times I_{\max} + 35.727 \tag{7}$$

$$\theta = 0.019521 \times I_{\max} + 43.672 \tag{8}$$

$$\theta = 0.018767 \times I_{\max} + 39.744 \tag{9}$$

$$\theta = 0.018844 \times I_{\max} + 34.039 \tag{10}$$

$$\theta = 0.006478 \times I_{\max} + 45.658 \tag{11}$$

$$\theta = 0.006221 \times I_{\max} + 41.983 \tag{12}$$

$$\theta = 0.006238 \times I_{\max} + 36.714 \tag{13}$$

According to the figures and corresponding equations, the coefficient of $I_{\max}$ is relative to the different transformer ratios. It is easily noticed that the coefficient is only relative to the number of winding in primary coil. The approximate mapping for three different numbers of winding 300,000, 200,000, and 100,000 are 0.018, 0.012, and 0.006, respectively. It means that under this configuration, the numbers of winding in the primary coil proportionally correspond to the above coefficients, while the number of winding in the secondary coil is little relative to the different situation.

This rule can be used to serve the current welding control strategy. We can set a scaling factor for presenting the ratio of the winding number in the primary coil when different transformers are employed, and then a corresponding conduction angle θ can be easily obtained. Hence, the predetermined selected control criteria, which is described as I^2t, can be transformed as the corresponding welding current I which caters to the new welding condition. Then, the corresponding constant current control method is conducted to guarantee that the practical I^2t is approaching the predetermined selected one.

4 Simulation and analysis

To validate above deduction and explore how to employ this method in reality, corresponding simulations were conducted. The simulation was based on MATLAB Simulink shown in Fig. 4, which has the same electrical structure as the actual system used in the RSW machine. Firstly, the varying workpiece resistance, which was dynamic resistance, should be seriously considered. According to the dynamic resistance characteristics during the resistance spot welding process [27, 28], a typical dynamic resistance curve was employed in the simulations, which is shown in Fig. 8.

In the simulation, the corresponding values when the primary and secondary windings were respectively 200,000 and 3000 were employed as a reference. In addition, 5000A of the RMS value of the welding current was used as the constant welding current. Under this circumstance, the actual welding

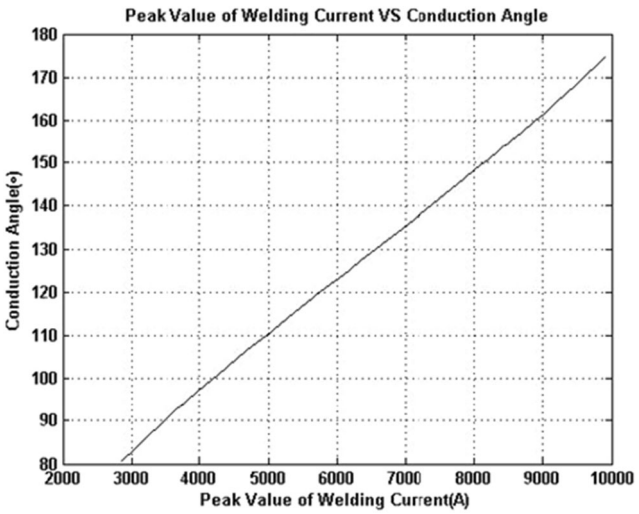

Fig. 5 Peak value of the welding current VS conduction angle (winding 200,000/3000)

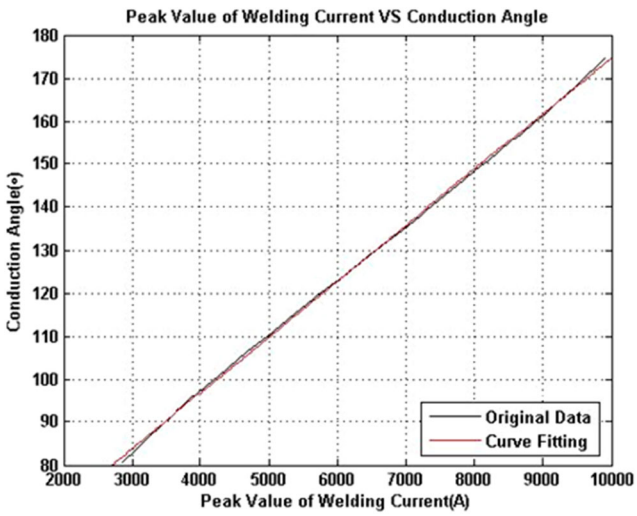

Fig. 6 Curve fitting result of data in Fig. 5

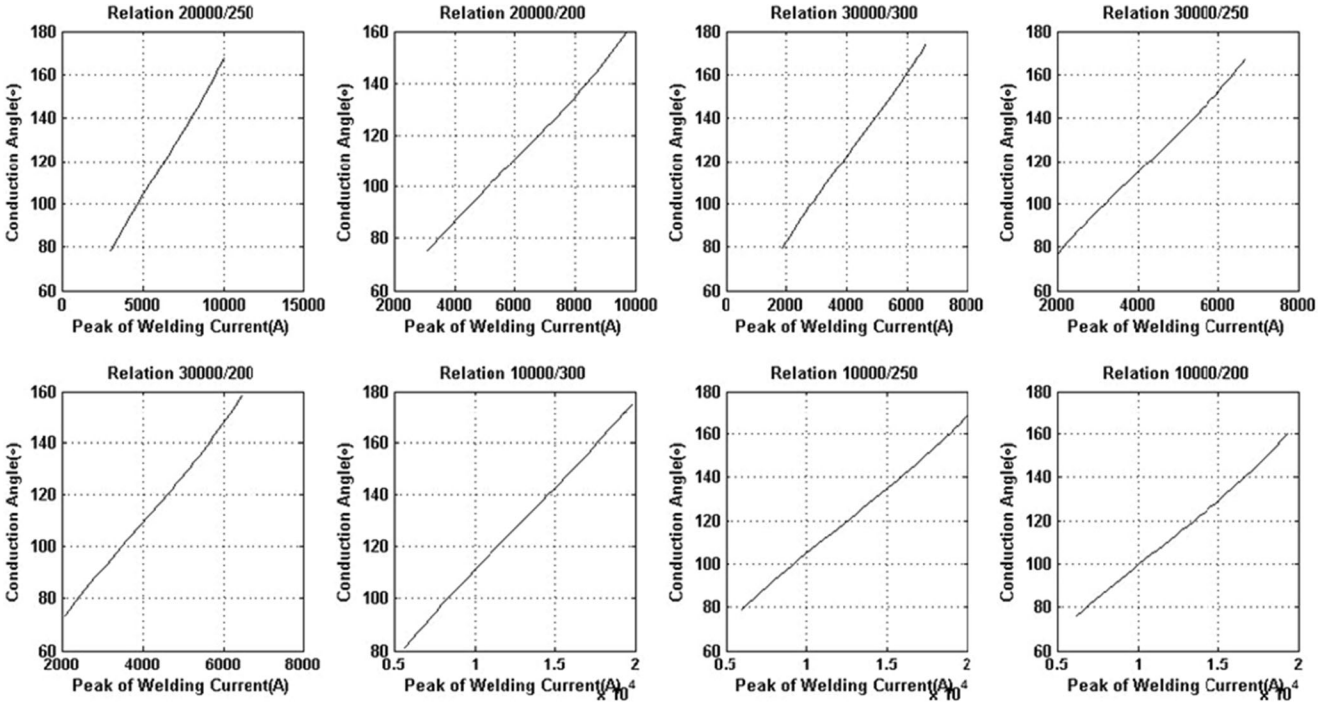

Fig. 7 Relation between θ and I_{max} in different ratios of the windings

current and the values of I^2t in the 12 control cycles are depicted as shown in Fig. 9.

Other welding machines may have different windings, for example, when the primary and secondary windings were respectively 100,000 and 2500, and then the 5000 of the welding current should correspondingly change, because the value of I^2t can have a difference. Due to the dynamic resistance of the workpiece, an approximately the same trend follows; in the simulation, the dynamic resistance was assumed to have the same variation. Figure 10 shows the actual welding current and the values of I^2t, when the winding is 100,000/2500 and the constant welding current is 5000A.

It can be seen that the constant current control can fulfill the expectance; however, the values of I^2t had a large difference when compared to Fig. 9, which shows that the constant welding current must be changed when winding ratios are different.

According to Eqs. (5) and (12), which respectively corresponded to 200,000/3000 and 100,000/2500 of windings, to conveniently analyze the process, the two equations can be re-written as follows:

$$\begin{cases} \theta_1 = 0.012975 \times I_{max1} + 44.929 \\ \theta_2 = 0.006221 \times I_{max2} + 41.983 \end{cases} \quad (14)$$

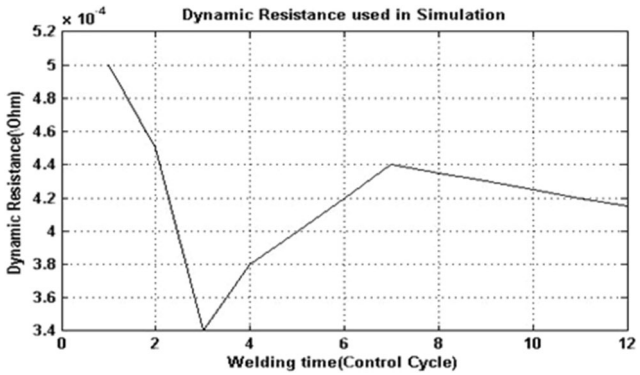

Fig. 8 A typical dynamic resistance curve used in the simulation

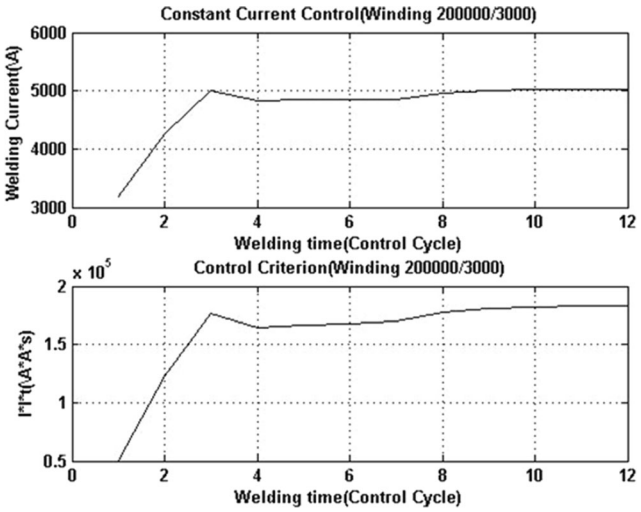

Fig. 9 Actual welding current and the values of I^2t (winding 200,000/3000)

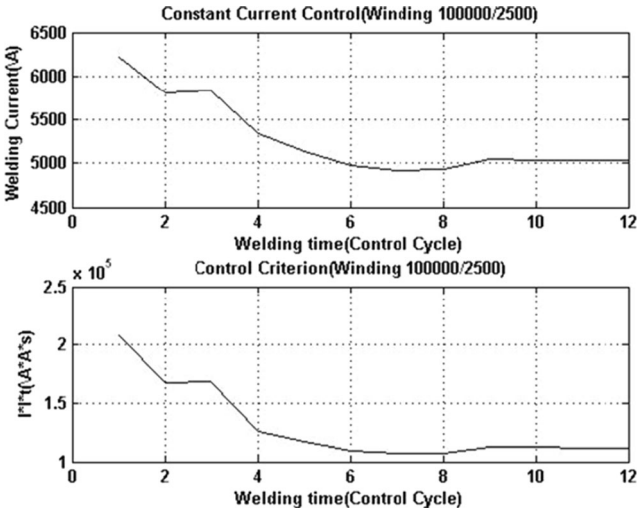

Fig. 10 Actual welding current and the values of I^2t (winding 100,000/2500)

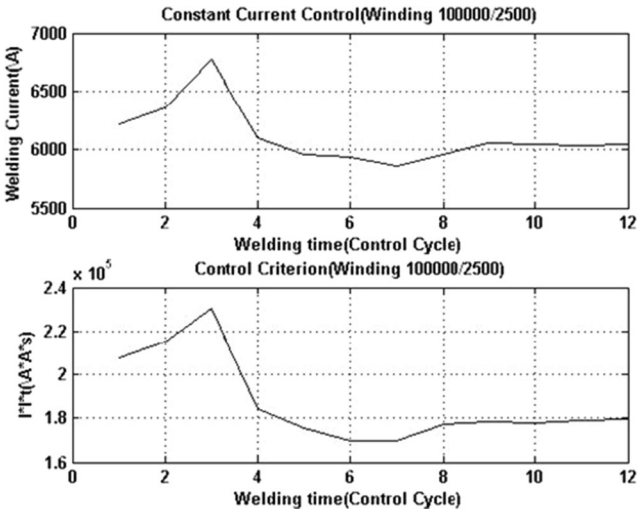

Fig. 11 Actual welding current and the values of I^2t after revising the welding current (winding 100,000/2500)

Subscript 1 denotes the relation when the windings were 200,000/3000, while subscript 2 denotes the relation when the windings were 100,000/2500. We want to obtain a corresponding I_{RMS2}, which can make the value of I^2t in Fig. 10 equal to the same item in Fig. 9. The corresponding value of I_{RMS1} was 5000A. If the values of I^2t obtained by two windings had little difference, the conduction angle θ may have little difference; hence, θ_2–41.983 may be approximately equal to θ_1–44.929 and the effects of the difference can be ignored. In addition, we supposed that a constant coefficient exists between the RMS value of welding current and the maximum of the welding current. Therefore, the following equation can be deducted:

$$\frac{I_{RMS2}^2}{I_{RMS1}^2} = \frac{0.012975}{0.006221} \approx 2 \tag{15}$$

Then, it can be obtained that

$$I_{RMS2} \approx \sqrt{2} I_{RMS1} \tag{16}$$

Moreover, under this circumstance, we hope to change the value of I to make the I^2t reasonable; directly using this change may induce errors. For convenience, a modified coefficient was employed

$$I_{RMS2} = k_1 \sqrt{2} I_{RMS1} \tag{17}$$

where k_1 is a coefficient, after several trials, we set $k_1 = 0.85$ in this simulation. Hence, the constant welding current in 100,000/2500 of windings can be set to $5000 \times \sqrt{2} \times 0.85$ instead of 5000. The corresponding results can be shown in Fig. 11.

Though the values of I^2t still were different from the corresponding figure in Fig. 9, it was more reasonable than that in Fig. 10. Because some assumptions were employed in the simulation, it is difficult to obtain absolutely the same results as shown in Fig. 9.

In addition, other windings can also be employed to validate the proposed method. The combination of the windings which were 300,000/3000 was chosen. Directly changing the winding ratio can be obtained in the following results as shown in Fig. 12.

Then, the same measures can be taken in this ratio. Corresponding equations can be re-written as follows:

$$\begin{cases} \theta_1 = 0.012975 \times I_{max1} + 44.929 \\ \theta_3 = 0.019521 \times I_{max3} + 43.672 \end{cases} \tag{18}$$

Then, the relation between two currents can be calculated as follows:

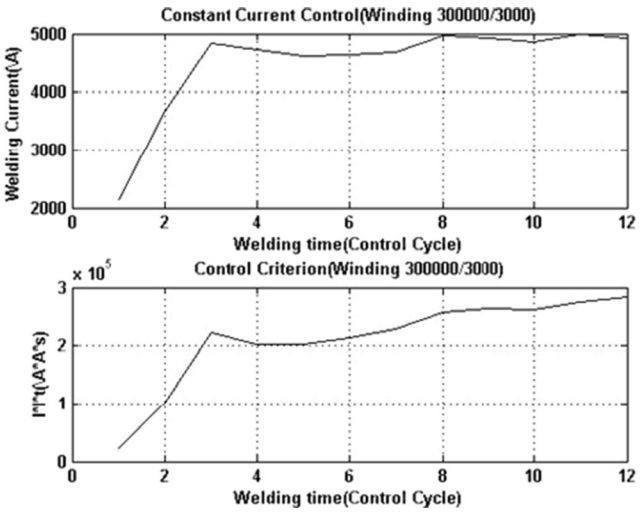

Fig. 12 Actual welding current and the values of I^2t (winding 300,000/3000)

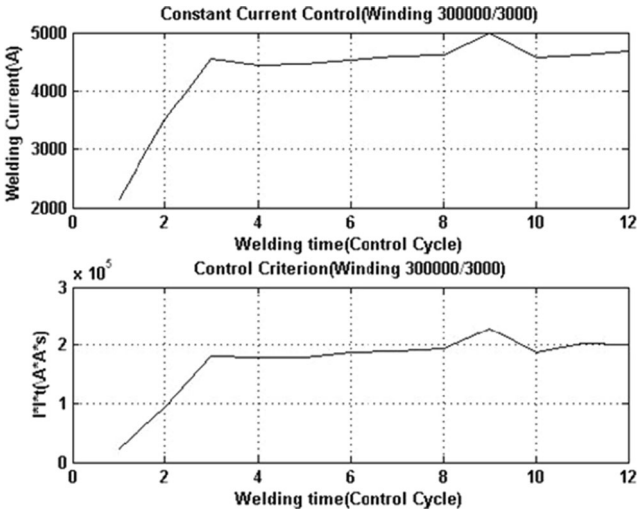

Fig. 13 Actual welding current and the values of I^2t after revise the welding current (winding 300,000/3000)

$$I_{\mathrm{RMS3}} = k_2\sqrt{2/3}I_{\mathrm{RMS1}} \tag{19}$$

After several trials, the modified coefficient can be set to be 1.15; then, the constant welding current in 300,000/3000 of windings can be set to $5000\times\sqrt{2/3}\times 1.15$ instead of 5000. The corresponding results can be shown in Fig. 13.

These results can present that changing the constant welding current can make the two welding machines which have different windings ratios obtaining fairly the similar results. It can supply a clue for developing a universal uniform energy delivery control strategy in practical welding productions.

Because the above simulations were based on the visual electrical environment provided by MATLAB Simulink instead of just equations solving or other relative methods, Simulink can simulate the actual welding process and provide convinced results, and it could be equivalent to the actual experiments. The simulation results were reliable and sufficient for instructing the actual applications.

5 Conclusion

Developing a general energy control strategy is very important to assure uniform welding quality during practical welding operations. After a detailed analysis of the resistance of the spot welding process, I^2t can be considered as an ideal controllable constant variable which can guarantee the uniform energy delivery to assure the uniform welding quality. However, it is a compound variable which is difficult to control in reality. Under the circumstance, the constant welding current can replace it in an actual controller design. The welding transformer is an important component in the welding machine. The difference of windings in primary and secondary coils of the transformer may induce the same welding current, but correspond to a different value of I^2t. Through simulating the welding process, the rules between peak value of the welding current and the conduction angle, which is also a duration of the welding current in one control cycle, can be obtained, then it can be observed that the coefficient between the two parameters is relative to the windings in the primary coil. This characteristic can be employed to obtain the corresponding constant welding current when transformers with different winding ratios are employed. Corresponding simulations and comparisons were conducted to validate the proposed method. Though the work was based on the single-phase AC RSW machine, the same principle and idea can be employed in the three-phase medium-frequency DC RSW machine.

In this work, the simulations using MATLAB Simulink were employed to conduct and validate the proposed method. Though the actual experiments were not conducted, the simulation used the visual electrical model instead of mathematical equations, the phenomena were observed and it can be confirmed that the proposed method can be definitely validated. In the future, we will continue to develop more general energy control strategy based on this method so as to facilitate the current welding production and improve the practical efficiency.

Acknowledgements The project is supported by Natural Science Foundation of China (Grant No: 51605103), Natural Science Foundation of Guangdong Province (Grant No: 2015A030313663) and Public Welfare Research and Capacity Building Project of Guangdong Province (Grant No: 2015A010104010).

Reference

1. Robert J, Messler W, Jou M (1996) Review of control systems for resistance spot welding:past and current practices and emerging trends. Science and Technology of Welding & Joining 1(1):1–9
2. El-Banna M (2015) A novel approach for classifying imbalance welding data: Mahalanobis genetic algorithm. Int J Adv Manuf Technol 77(1–4):407–425
3. Liu J, Xu G, Ren L, Qian Z, and Ren L (2016) "Defect intelligent identification in resistance spot welding ultrasonic detection based on wavelet packet and neural network (online first)," *International Journal of Advanced Manufacturing Technology,* pp. 1–8
4. Zhang H, Hou Y, Zhang J, Qi X, Wang F (2015) A new method for nondestructive quality evaluation of the resistance spot welding based on the radar chart method and the decision tree classifier. Int J Adv Manuf Technol 78(5–8):841–851
5. Wan X, Wang Y, Zhao D (2016) Quality monitoring based on dynamic resistance and principal component analysis in small scale resistance spot welding process. Int J Adv Manuf Technol 86: 3443–3451
6. Podrz˙aj P, Polajnar I, Diaci J, Kariz Z (2008) Overview of resistance spot welding control. Sci Technol Weld Join 13(3):215–224

7. Li W, Cerjanec D, Grzadzinski GA (2005) A comparative study of single-phase AC and multiphase DC resistance spot welding. J Manuf Sci Eng 127(3):583–589
8. Brown BM (1987) A comparison of AC and DC current in the resistance spot welding of automotive steels. Weld J 66(1):18–23
9. Nied HA (1984) The finite element modeling of the resistance spot welding process. Weld J 63(4):123s–132s
10. Eisazadeha H, Hamedib M, Halvaeec A (2010) New parametric study of nugget size in resistance spot welding process using finite element method. Mater Des 31(1):149–157
11. Zhou K, Cai L (2014) On the development of nugget growth model for resistance spot welding. J Appl Phys 115:164901.1–16490112
12. Kas Z and Das M (2014) "A thermal dynamical model based control of resistance spot welding," in Electro/Information Technology (EIT), 2014 I.E. International Conference on, 5–7, pp. 264–269
13. Gedeon S, Sorensen C, Ulrich K, Eagar T (1987) Measurement of dynamic electrical and mechanical properties of resistance spot welds. Weld J 66(2):378s–385s
14. Cho Y, Rhee S (2004) Quality estimation of resistance spot welding by using pattern recognition with neural networks. Instrumentation and Measurement, IEEE Transactions on 53(2):330–334
15. Cho Y, Rhee S (2000) New technology for measuring dynamic resistance and estimating strength in resistance spot welding. Meas Sci Technol 11(8):1173–1178
16. Araki K, Chen X, Chen J, Ishino Y, and Mizuno T (1996) "Application of a model reference fuzzy adaptive control to the spot welding system," in *SICE '96. Proceedings of the 35th SICE Annual Conference*, pp. 1139–1144
17. Zhang Y, Chen G, Lin Z (2004) Study on weld quality control of resistance spot welding using a neuro-fuzzy algorithm. Lect Notes Comput Sci 3215/2004:544–550
18. Lai X, Zhang X, Zhang Y, Chen G (2007) Weld quality inspection based on online measured indentation from servo encoder in resistance spot welding. Instrumentation and Measurement, IEEE Transactions on 56(4):1501–1505
19. Zhou K, Cai L (2013) Online nugget diameter control system for resistance spot welding. Int J Adv Manuf Technol 68(9–12):2571–2588
20. Zhou K and Cai L (2012) "On current control method for single-phase AC resistance spot welding," in *19th IEEE International Conference on Electronics, Circuits, and Systems*, Seville, Spain, , pp. 857–860
21. Williams NT, Parker JD (2004) Review of resistance spot welding of steel sheets part 1 modelling and control of weld nugget formation. Int Mater Rev 49(2):45–75
22. Zhou K, Cai L (2014) A nonlinear current control method for resistance spot welding. IEEE /ASME Transactions on Mechatronics 19(2):559–569
23. El-Banna M, Files D, Chinnam RB (2008) Online qualitative nugget classification by using a linear vector quantization neural network for resistance spot welding. Int J Adv Manuf Technol 36(3–4):237–248
24. Gong L and Liu CL (2006) "Dynamic power factor measurement in A.C. resistance spot welding with embedded ANN " in *Industrial Informatics, 2006 I.E. International Conference on*., pp. 1183–1188
25. Duan B, Zhang C, Guo M, Zhang G (2015) A new digital control system based on the double closed-loop for the full-bridge inverter. Int J Adv Manuf Technol 77(1–4):241–248
26. Zhou K, Cai L (2014) Study of safety operation of AC resistance spot welding system. IET Power Electron 7(1):141–147
27. Dickinson DW, Franklin JE, Stanya A (1980) Characterization of spot welding behavior by dynamic electrical parameter monitoring. Weld J 59(6):170s–176s
28. Tan W, Zhou Y, Kerr HW, Lawson S (2004) A study of dynamic resistance during small scale resistance spot welding of thin Ni sheets. J Phys D Appl Phys 37(14):1998–2008